

$q_1$  and  $q_2$  and  $t_1$  and  $t_2$  and observing that  $\log(e - q_1)/(e - q_2) = \log(v_1/v_2) = (\Delta \log v)$  for the interval  $(\Delta t)$  (1, 8, 9), gives

$$\frac{1}{i} = \frac{\Delta t}{2.303 \Delta \log v} \frac{k_p}{K_a} - \frac{1}{K_a} \quad (6)$$

The ratio  $k_p/K_a$  has the dimensions of the bimolecular rate constant  $[\text{min}^{-1}(\text{mole/liter})^{-1}$ , or  $\text{min}^{-1}M^{-1}]$ . If the value of  $K_a$  from Eq. 3 is substituted into Eq. 5 and we place

$$k_i = k_p/K_a \quad (7)$$

then

$$dq/dt = k_i(e - q - r)i \quad (8)$$

The expression for the rate of inhibition proposed earlier by Aldridge (1) is

$$dq/dt = k_i(e - q)i \quad (9)$$

where direct interaction of  $E$  and  $I$  to form  $(EI)_q$  is assumed.

The dimensions of the  $k_i$  terms in Eqs. 8 and 9 are the same, but the two constants have different meanings. The  $k_i$  in Eq. 9 is evidently a simple rate constant. The  $k_i$  of Eq. 8 has a more complex meaning as given by Eq. 7 and includes an equilibrium as well as a rate constant, and the term *rate* should therefore not be applied. Since both  $k_i$  terms govern the same reaction sequence and the term *bimolecular rate constant* is widely accepted in this context, it is suggested that the  $k_i$  of Eq. 8 be called the *bimolecular reaction constant*.

Substitution of Eq. 7 into Eq. 6 gives

$$\frac{1}{i} = \frac{\Delta t}{2.303 \Delta \log v} k_i - \frac{1}{K_a} \quad (10)$$

Equation 10 was derived on the assumption of a reversible step and on the observation that the inhibition reaction is first-order when  $i$  is constant. But  $i$  can be varied for different experimental reactions and yet remain constant over the course of any individual reaction. Equation 10 can then be applied experimentally since various values of  $(\Delta t/2.303 \Delta \log v)$  can be determined for corresponding values of  $(1/i)$ . Values of  $(\Delta t/2.303 \Delta \log v)$  are obtained from a plot of  $\log v$  against  $t$  at constant  $i$ . According to Eq. 10, the plot of  $(1/i)$  against  $(\Delta t/2.303 \Delta \log v)$  will be linear. The slope will be  $k_i$ , the intercept on the  $(1/i)$  axis will be  $(-1/K_a)$ , and the intercept on the  $(\Delta t/2.303 \Delta \log v)$  axis will be  $(1/k_p)$ .

Intersection of the axes in the predicted quadrants by the extrapolated line would support the assumption of a

reversible intermediate, as well as providing a means of evaluating  $k_p$  and  $K_a$ . If no reversible step occurred, the line would pass through the origin, but for this to be conclusive, the supporting experiment would have to include values of  $i$  and  $t^{-1}$  of an order which could reasonably be assigned to  $K_a$  and  $k_p$ .

Preliminary experiments were carried out using diisopropyl phosphorofluoridate (DFP) and malaoxon, (*O*, *O*-dimethyl S [1,2-dicarboethoxyethyl] phosphorothiolate) as inhibitors and a commercial preparation of human serum cholinesterase (10). Inhibitor and enzyme solutions were mixed and allowed to react from 0.5 to 3 minutes at pH 7.6, 37°C. Inhibition was stopped and the residual activity was measured by adding the mixture to a solution of acetylcholine substrate. The procedure has been described in detail (9).

The results were plotted according to Eq. 10 and are shown in Fig. 1. Both plots are reasonably linear. Extrapolation of the line for malaoxon gave intercepts from which significant values of  $k_p$  and  $K_a$  were calculated, but the intercepts of the line for DFP were too close to the origin to be of real significance. The results with malaoxon supported the proposed treatment. Because of experimental limitations those with DFP were inconclusive.

A value for  $k_i$  can be calculated for each point in Fig. 1 either by the equation of Aldridge (1), where

$$k_i = \frac{2.303 \Delta \log v}{\Delta t} \frac{1}{i} \quad (11)$$

or by rearranging Eq. 10, from which

$$k_i = \frac{2.303 \Delta \log v}{\Delta t} \left( \frac{1}{i} + \frac{1}{K_a} \right) \quad (12)$$

When calculated by Eq. 11,  $k_i$  values for malaoxon inhibition increased progressively from  $7.7 \pm 0.4 \times 10^8$  to  $1.36 \pm 0.12 \times 10^4 M^{-1} \text{min}^{-1}$  as  $i$  increased over the range,  $5 \times 10^{-4}$  to  $5 \times 10^{-5} M$ . The average  $k_i$  was  $1.17 \pm 0.25 \times 10^4 M^{-1} \text{min}^{-1}$ . When calculated by Eq. 12, from the value of  $K_a$  obtained graphically ( $7.7 \times 10^{-4} M$ ), the average was  $1.42 \pm 0.11 \times 10^4 M^{-1} \text{min}^{-1}$  and  $k_i$  did not vary significantly with change in  $i$ .

A similar analysis for DFP gave an average  $k_i$  of  $4.18 \pm 0.71 \times 10^6$  and a lowest value of  $2.96 \pm 0.34 \times 10^6 M^{-1} \text{min}^{-1}$  at the highest DFP concentration ( $2 \times 10^{-5} M$ ). These differences were barely significant, but together with the intercept values they suggested  $K_a$  and  $k_p$  values in the order of  $1 \times 10^{-5} M$  and  $30 \text{min}^{-1}$ .

Determination of  $k_i$  based on Eq. 11 is then valid only when  $K_a$  is several times  $i$ , and the present results suggest that  $k_i$  should be determined over a range of inhibitor concentrations. In addition, the present treatment or indeed that of Aldridge (1) should only be applied if the plots of  $\log v$  against  $t$  are reasonably linear.

A. R. MAIN

Pesticide Research Laboratory, North Carolina State University, Raleigh

#### References and Notes

1. W. N. Aldridge, *Biochem. J.* **46**, 451 (1950).
2. L. P. Hammett, *Physical Organic Chemistry* (McGraw-Hill, New York, 1940), pp. 186-198.
3. T. R. Fukuto, R. L. Metcalf, M. Y. Winston, R. B. March, *J. Econ. Entomol.* **56**, 808 (1963).
4. R. D. O'Brien, *Toxic Phosphorus Esters* (Academic Press, New York, 1960), pp. 83-99.
5. J. F. Mackworth and E. C. Webb, *Biochem. J.* **42**, 91 (1948); A. J. J. Ooms, A. Hansen, L. Ginjaar, *Proc. Intern. Congr. Biochem.* **4th**, Vienna, 1958 (Pergamon, New York, 1960), vol. 15, p. 37, Sect. 4-6.
6. W. N. Aldridge, *Biochem. J.* **54**, 442 (1953); J. E. Casida, *J. Agr. Food Chem.* **4**, 772 (1956); K. Van Asperen and H. M. Dekhuijzen, *Biochim. Biophys. Acta* **28**, 63 (1958).
7. J. L. Krysan and L. E. Chadwick, *Entomol. Exptl. Appl.* **5**, 179 (1962).
8. A. R. Main and W. C. Dauterman, *Nature* **198**, 551 (1963).
9. ———, in preparation.
10. Malaoxon was prepared by Dr. W. C. Dauterman of this laboratory. Partially purified human serum cholinesterase was purchased from Sigma Chemical Co., St. Louis, Mo. DFP was purchased from Mann Research Laboratories, New York. I thank Mrs. W. Hobbs and Mrs. R. Reynolds for help. Supported in part by USPHS grant EF-415. Contribution from the Pesticide Research Laboratory, North Carolina Agricultural Experiment Station, Raleigh. Published with the approval of the director of research. Paper No. 1771 of the journal series.

11 March 1964

#### Distribution of Narrow-Width Magnetic Anomalies in Antarctica

Abstract. Data for aeromagnetic profiles obtained in Antarctica during the 1963-64 austral summer were used together with earlier results to construct a map showing the areal distribution of narrow-width magnetic anomalies. Numerous anomalies are associated with known volcanic mountains in western Antarctica. A large area of few anomalies is probably a result of an extension of the thick metasedimentary section observed in the Ellsworth Mountains. Portions of the Trans-Antarctic Mountains have associated anomalies which are probably caused by late Cenozoic volcanic rocks.

Two field investigators (1) from the University of Wisconsin flew approximately 48,000 km of aeromagnetic profiles in Antarctica from November 1963 through January 1964. They used

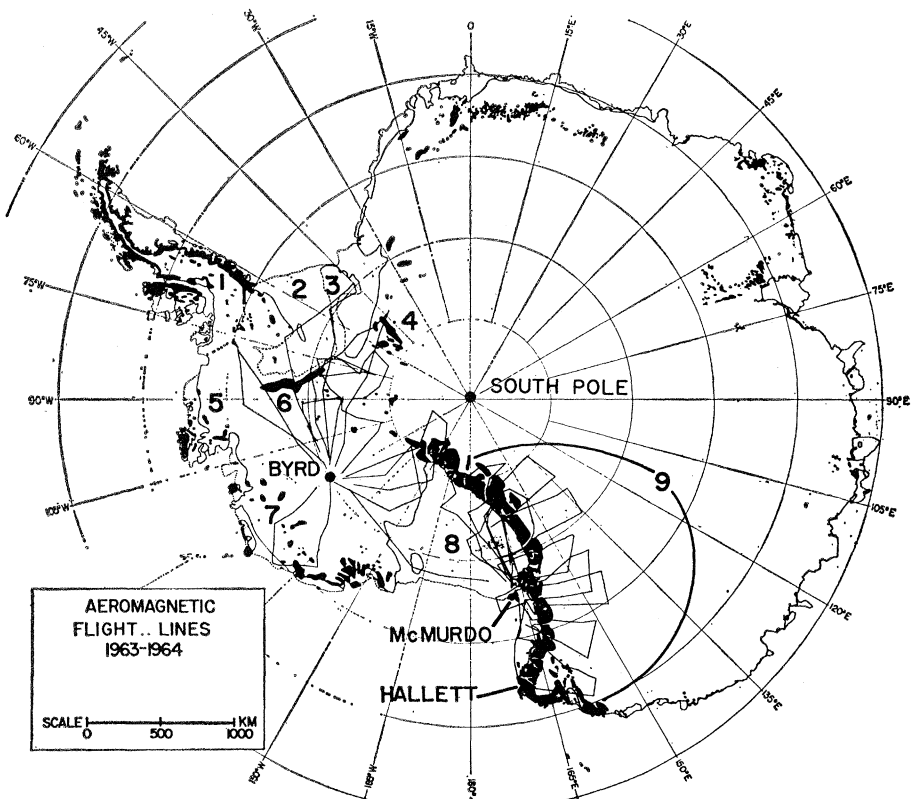


Fig. 1. Index map showing flight tracks for the 1963-64 season. Place locations: 1, Antarctic Peninsula; 2, Filchner Ice Shelf; 3, Berkner Island; 4, Pensacola Mountains; 5, Ellsworth Land; 6, Ellsworth Mountains; 7, Marie Byrd Land; 8, Ross Ice Shelf; and 9, Trans-Antarctic Mountains.

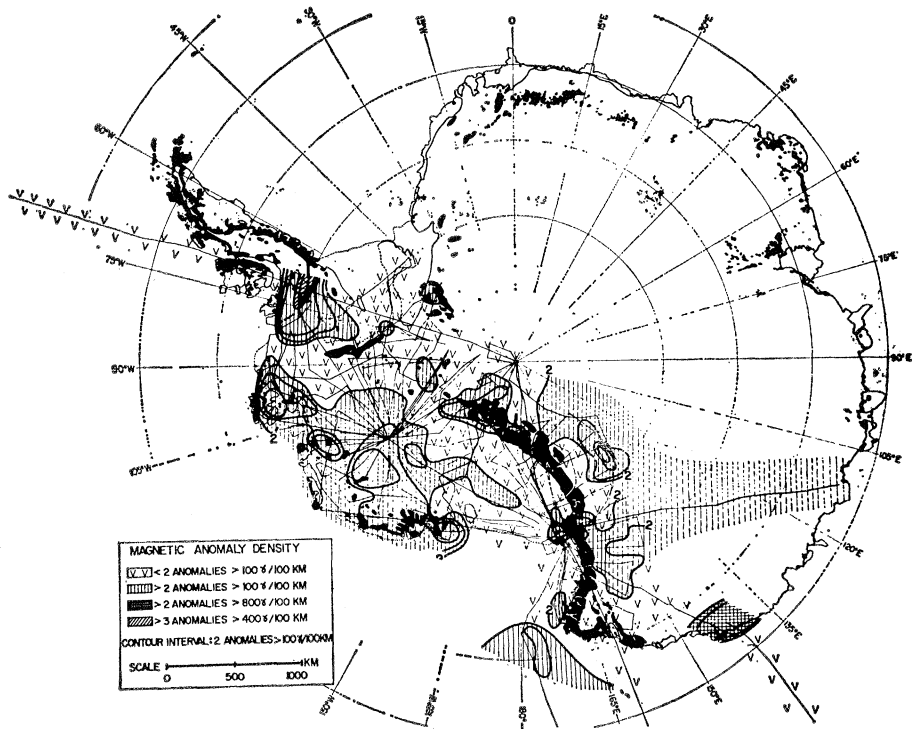


Fig. 2. Areal distribution of magnetic anomalies with total intensities less than 50 km in width. Average density for total area shown with less than two anomalies of 100 gamma or greater amplitude per 100 km of track is 0.6 anomalies per 100 km.

two digital recording proton precession magnetometer systems (2) to measure total intensity from U.S. Navy DC-3 aircraft; flights originated from McMurdo and Byrd stations. Flight altitudes ranged from 500 to 1000 m above the snow surface, although occasionally weather and terrain forced the aircraft higher. Elevations of the aircraft and snow surface were measured with aneroid and radio altimeters. Magnetograms for diurnal corrections were obtained from Scott Base (at McMurdo Sound) and South Pole, Hallett, and Byrd stations.

Figure 1 shows the flight tracks. About 28,000 km of traverses were flown in the Trans-Antarctic Mountains area roughly perpendicular to the strike of the range and extending over the ice sheet of eastern Antarctica about 450 km beyond the front of the range. These traverses penetrated the range via the following glaciers from north to south: Ironside (72°S, 169°E), Campbell, Reeves, Davis, Mawson, Mackay, Ferrar, Skelton, Darwin, Byrd, Nimrod, Lennox King, Beardmore, Liv, Robert Scott, and an unnamed glacier at 86°S, 136°W. Another 20,000 km of flight lines were concentrated to the east of Byrd Station over the northern Pensacola Mountains, Berkner Island, the Filchner Ice Shelf, and the Ellsworth Mountains.

These data together with aeromagnetic data for 27,000 km collected previously by workers at the University of Wisconsin from 1958 to 1961 (3) and with data for 13,000 km collected during Project Magnet (4) were used to construct the anomaly density map shown in Fig. 2. This map shows the distribution of anomalies with widths less than 50 km which were determined from the profiles by drawing a smoothed regional curve through the data. Amplitudes and positions of anomalies were plotted on maps. The numbers of anomalies per 100 km of flight line greater than 100, 400, and 800 gamma (1 gamma = 10<sup>-6</sup> oersted) were determined for squares of approximately 1° of latitude length of side. The mean values for the squares were contoured as shown in Fig. 2.

This map shows a rather complex distribution of magnetic rock. Many anomalies are associated with the volcanic rocks studied in Marie Byrd Land, Ellsworth Land, and the Southern Antarctic Peninsula (5) and give an indication of the subglacial extent of these highly

magnetic rocks. South of these areas in western Antarctica the terrane is generally quite devoid of anomalies, with occasional exceptions. This is probably the result of sedimentary or metasedimentary rock, since 14 km of metasediments were reported in the Sentinel Range (6). The dividing line between this sedimentary province and the volcanic areas to the northwest and the Antarctic Peninsula is quite abrupt and can be traced reasonably accurately from profile to profile. It appears likely that the sedimentary rock extends east beneath the Filchner Ice Shelf.

The Trans-Antarctic Mountains have areas of numerous anomalies of narrow width and other areas with essentially smooth fields. It is quite possible that the anomalous areas are caused by the McMurdo volcanics (7) of late Cenozoic age. The dolerite sills (7) intruding into the late Paleozoic-Mesozoic Beacon system do not have susceptibilities high enough to produce the observed anomalies (8). The flight from McMurdo to Wilkes shows a number of anomalies which are probably associated with ancient intrusive or extrusive rocks of the pre-Cambrian shield in this area. The highest anomalies observed in Antarctica occur in the area around 67°S, 140°E. The Project Magnet flight in this area recorded one anomaly with an amplitude of about 3500 gamma.

JOHN C. BEHRENDT \*

*Geophysical and Polar Research Center,  
University of Wisconsin, Madison*

#### References and Notes

1. Per Gjelsvik and Richard E. Wanous.
2. R. J. Wold, *Univ. of Wisconsin Geophysical and Polar Research Center Rept. 64-4*, in press; Elsec-Wisconsin digital recording systems.
3. J. C. Behrendt and R. J. Wold, *J. Geophys. Res.* **68**, 1145 (1963); N. A. Ostenson and E. Thiel, in preparation.
4. Data furnished by the U.S. Naval Oceanographic Office.
5. G. A. Doumani and E. G. Ehlers, *Bull. Geol. Soc. Am.* **73**, 877 (1962); C. Craddock, T. W. Bastien, R. H. Rufford, *Polar Record*, abstr. 756 (1963); J. C. Behrendt, *J. Geophys. Res.* in press.
6. C. Craddock, J. J. Anderson, G. F. Webers, paper presented at the symposium of the Scientific Committee on Antarctic Research, Capetown, 1963.
7. B. M. Gunn, and G. Warren, *New Zealand Geol. Survey Bull.* **71** (1962).
8. G. Bull, E. Irving, I. Willis, *Geophys. J.* **5**, 320 (1962).
9. This work was supported by an NSF grant to the University of Wisconsin. The CDC 1604 computer of the University of Wisconsin Numerical Analysis Laboratory was used in the data processing. Air Development Squadron 6 (VX-6), U.S. Navy, capably carried out the flight program. Geophysical and Polar Research Center contribution No. 133.

\* Present address: U.S. Geological Survey, Denver, Colo.

30 March 1964

22 MAY 1964

## Radiocarbon Dating of Bone and Shell from Their Organic Components

*Abstract. A method of dating bone and shell by radiocarbon content has been developed. The mineral is removed by mild acid treatment and the residual carbon is dated in the usual manner.*

Until recently, the radiocarbon dating of archeological bone samples was based primarily on the dating of associated charcoal, and in some cases on the natural calcium carbonate contents of bones. However, dates by correlation with charcoal may not always be correct. Even greater doubts exist on the accuracy of dates based on calcium carbonate which may have been replaced by ground-water carbonate of varying age.

It is now possible to date bones directly from their content of organic carbon or collagen (1). There is no known natural mechanism by which collagen may be altered to yield a false age.

Generally dry modern bone is composed approximately of 50 percent calcium phosphate, 10 percent calcium carbonate, 25 percent collagen, and 5 to 10 percent bone fat, and the remainder is made up mainly of mucopolysaccharides, calcium fluoride, magnesium phosphate, sodium salts, and heavy elements such as iron and manganese.

Collagen is characterized chemically as a protein with a low content of aromatic amino acids and a high content of pyrrolidine amino acids (proline and hydroxyproline) as well as glycine. Also, it is specifically hydrolyzed by the enzyme collagenase. Collagen is found as fibrils 0.3 to 0.5  $\mu$  thick throughout bone. The individual fibrils are often collected into bundles of 3 to 5  $\mu$ . The physiological turnover of collagen is very slow as determined by isotopic measurements. Bone collagen is chemically indistinguishable from the collagen in cartilage, skin, and tendon.

The bone mineral is composed of crystals of chiefly calcium phosphate with the structure of a hydroxyapatite  $[\text{Ca}_3(\text{PO}_4)_2]_3 \cdot \text{Ca}(\text{OH})_2$ . The crystals are oriented along the major axis of the collagen fibrils. Roughly speaking, bone has the structure of a brick wall. The bricks are apatite; the mortar consists of citrate, carbonate, and other ions; and the collagen fibers act as reinforcing strands in the loosely assembled intercrystalline matrix.

There have been attempts to use the carbonate portion of bones for radiocarbon dating by liberating carbon dioxide with hydrochloric acid. However, one may arrive very easily at fallacious dates because ground water contains atmospheric carbon dioxide of modern carbon-14 age. This carbonate can be exchanged with radioactively dead carbonate in the soil (limestone). Therefore, ground-water carbonate may possess a radiocarbon age of anywhere from 0 to 5730 years (50-percent exchange). Theoretically, bones immersed in modern carbonate water could be dated as being too young and bones in radioactively dead water as being too old. Since older bones have a much less preserved structure than young bones, the error will be most pronounced in older specimens owing to the possibility of greater exchange.

These considerations led to the dating of bones from their collagen—which does not suffer from exchange phenomena. However, the collagen content of bone decreases with age to such low concentrations that isolation of sufficient collagen for radiocarbon dating becomes difficult with the oldest bones. The oldest specimen that has been dated in this way had a collagen content of about 0.16 percent. It was about 9000 years old (UCLA-630). Unfortunately collagen does not decrease uniformly with age for finds around the world. For example, a 4000-year-old bone (UCLA-140) from Santa Rosa Island, California, buried in dry, permeable soil had a collagen content of about 15 percent whereas a 3300-year-old bone buried in moist English conditions had only 10 percent (1). When bones of different ages are found in the same general locality, they can be relatively dated, depending on their collagen content. Cook and Heizer were able to arrive at reasonably good absolute dates for bones derived from their collagen content for the general area of the southwestern United States (2).

Bones of the same age have a different collagen content in different environmental conditions in which they